EasyChair Preprint

№ 10404

Effect of Contact Angle Variation on Thermal Performance of Heat Pipe: Pore-Scale Numerical Simulation

Surendra Singh Rathore, Balkrishna Mehta, Pradeep Kumar and Mohammad Asfer

June 15, 2023

Effect of Contact Angle Variation on Thermal Performance of Heat Pipe: Pore-scale Numerical Simulation

Surendra Singh Rathore[1], Balkrishna Mehta[1], Pradeep Kumar[2]*, Mohammad Asfer[3]

[1] Department of Mechanical Engineering, IIT Bhilai, Raipur-492015, Chhattisgarh, India

[2] Numerical Experiment Laboratory (Radiation & Fluid Flow Physics), IIT Mandi, Mandi-175075, Himachal Pradesh, India

[3] Department of Mechanical Engineering, College of Engineering, Shaqra University, Shaqra-11911, Saudi Arabia

*pradeepkumar@iitmandi.ac.in

ABSTRACT

In the present study, a pore-scale simulation approach is used to analyze the heat and mass transfer processes in the heat pipe. Due to its topographic structure almost similar to the sintered wick structure used in the heat pipes, Triply-Periodic-Minimal-Surface (TPMS) based Fisher-Koch lattice is used for geometrical modelling of the porous wick structure for the first time. A relatively smaller heat load of 1000 W/m^2 is applied at the evaporator and condenser sections. Therefore, the effect of contact angle variation at solid-liquid-vapour interface is studied using the parameters like, temperature distribution, interface shape, and heat pipe limits (capillary, boiling, and entrainment), for heat transfer performance.

Keywords: Pore-scale simulation; Two-phase flow, TPMS lattice; Heat pipe.

1 Introduction

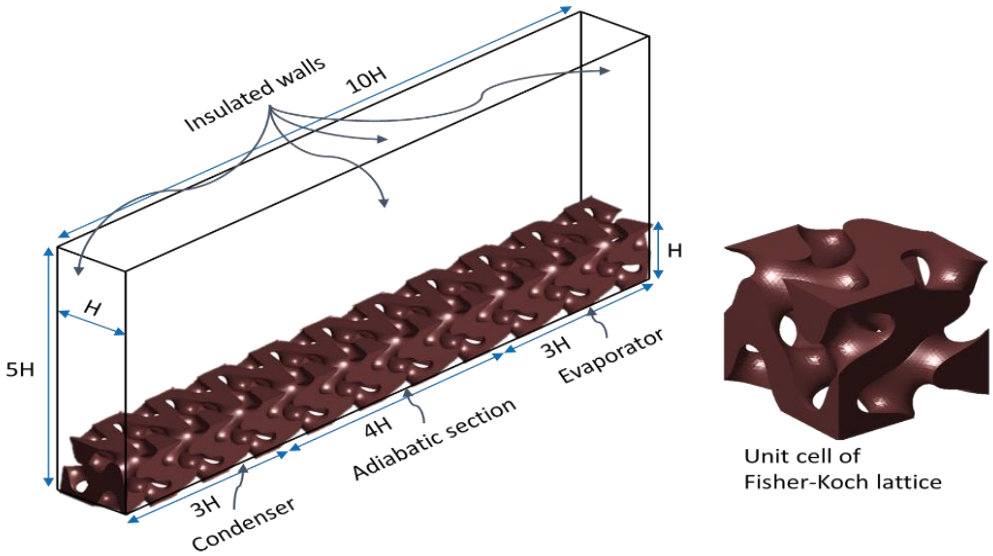

Figure 1: Schematic of rectangular heat pipe where regular porous structure of Fisher-Koch lattice is used.

In recent years, there has been an increasing demand for efficient and compact heat transfer devices capable of mitigating high thermal energy in various industries, including electronics cooling, aerospace applications, and energy conversion systems etc. Among the many innovative solutions developed, the heat pipes have emerged as a promising technology due to their ability to transfer heat over long distances with minimal temperature gradients [1, 2]. Understanding the underlying mechanisms that govern the thermal performance of heat pipes is crucial for optimizing their design and enhancing their efficiency [3, 4]. One critical factor influencing the performance of the heat pipes is the contact angle at the liquid-vapor interface within the capillary structure. The contact angle determines the shape and behavior of the meniscus, affecting the flow of the working fluid and the overall thermal conductivity of the heat pipe. While numerous studies have investigated the effect of various design parameters on the performance of heat pipes, the impact of contact angle variation on their thermal behavior has received relatively limited attention [5].

This paper aims to address the effect of contact angle variation on the thermal performance of the heat pipes through a comprehensive pore-scale simulation study. The proposed study employs advanced computational modeling techniques, allowing for detailed analysis and accurate predictions of the fluid flow behavior, phase change phenomena, and heat transfer characteristics within the wick's capillary structure.

2 Numerical Methodology

The Volume-of-Fluid (VOF) technique for two-phase flow simulation and Lee's model for liquid-vapour phase change are used in this work, which is carried out in the Ansys® Fluent CFD program. Taking one of the fluids as the primary phase (in our case, vapour), the mass source term accounts for the mass of vapour created or destroyed by vaporization or condensation, respectively. Similarly, the energy source term incorporates the heat absorbed or released. The surface force at the liquid-vapour interface is accounted in momentum conservation. Laminar flow model is applicable instead of turbulent models due of the system's small length-scale. Three dimensional transient governing equations for mass, momentum, and energy conservation are shown as follows:

$$\frac{\partial(\alpha_v)}{\partial t} + \nabla \cdot (\alpha_v \vec{u}) = \frac{\dot{m}_v}{\rho_v} \tag{1}$$

$$\frac{\partial(\rho \vec{u})}{\partial t} + \nabla \cdot (\rho \vec{u}\vec{u}) = -\nabla p + \mu \nabla^2 \vec{u} + \rho \vec{g} + \overrightarrow{F_s} \tag{2}$$

Where, α_v and ρ_v are the volume fraction and density of the vapour, $\vec{u}$ is the velocity vector and $\dot{m}_v$ is the mass source term which is calculated using the Lee's model. Moreover, the momentum balance contains the gravity ($\rho \vec{g}$) and surface tension ($\overrightarrow{F_s}$), along with the pressure ($-\nabla p$) and viscous forces ($\mu \nabla^2 \vec{u}$). Where, ρ and μ are fluid's density and dynamic viscosity and calculated using volume weighted average of liquid and vapour properties.

$$\frac{\partial(\rho h)}{\partial t} + \nabla \cdot (\rho h \vec{u}) = k \nabla^2 T + \dot{S}_e \tag{3}$$

The heat interactions due to diffusion ($k \nabla^2 T$), advection ($\nabla \cdot (\rho h \vec{u})$), and phase change ($\dot{S}_e$) are accounted in the energy conservation as shown in Eq. (3). Where, k and h are the thermal conductivity and enthalpy of the fluid calculated as the volume and mass weighted average of liquid and vapour properties, respectively.

$$\dot{m}_v = r \alpha_v \rho_v \frac{T - T_{sat}}{T_{sat}} \tag{4}$$

$$\dot{S}_e = -h_{lv} \dot{m}_v \tag{5}$$

In the Lee's model, mass and energy source terms described previously, are given in above equations (Eq. (4 and 5)). Here, T_{sat} is the saturation temperature (85 °C) and h_{lv} is the latent heat of vaporisation (2295.40 kJ/kg) of the fluid, calculated at the operating pressure of 0.57 bar. In addition, r is the mass transfer intensity factor, which must be selected from the range of values ($10^{-1} \leq r \leq 10^{7}$) to keep the interfacial temperature close to T_{sat}. Predicting a suitable value of r is one of the most challenging aspects of using Lee's model, and there are available benchmarks for this. The present numerical model

for the heat and mass transfer has also been validated using the Stefan and Film boiling problem and suitable value of mass transfer intensity factor is obtained around 10 sec^{-1}.
Furthermore, for pressure-velocity coupling, the SIMPLE algorithm is employed, and the Green-Gauss node-based scheme is used for the gradient calculations. The second order upwind and central differencing schemes are used for advection and diffusion terms, respectively. To compute the volume fraction and capture the interface location, high resolution interface construction (HRIC) method is utilized. The implicit formulation of second order is used for the temporal derivative. The continuity and momentum equations are converged up to the residuals 10^{-4} and 10^{-6}, respectively; however, the residual for the energy equation is 10^{-8}.
For the fluids, the properties of water (liquid and vapour) are used at saturation pressure 0.57 bar (T_{sat} = 85 °C), whereas for the solids, material properties of copper are used. The evaporator and condenser sections are provided with heat flux of 1000 W/m^2 for heating and cooling purpose, respectively. Remaining all external walls are kept thermally insulated. The internal walls where fluid is in contact are given the no-slip and thermally coupled boundary conditions, while the contact angle is varied as 20º, 40º, and 60º. Initially the liquid fills lower-half of the chamber height, while the vapour is accumulated at the upper-half.

3 Results and Discussion

3.1 Simulations

After performing the grid independent study, fixing the time size, and verifying the numerical model with the typical benchmarks, transient simulations are set up to run for variations of the contact angle. Fig. 2 shows the outcomes of the simulations after completion of 1 second. The temperatures at the heated (evaporator) and cooled (condenser) sections are not varying much from the saturation temperature (85 °C) and a deviation of ±0.2 °C is observed for the hot and cold surfaces. The accumulation of liquid is towards the condenser in higher contact angle and this gets decreased for the lower contact angle.

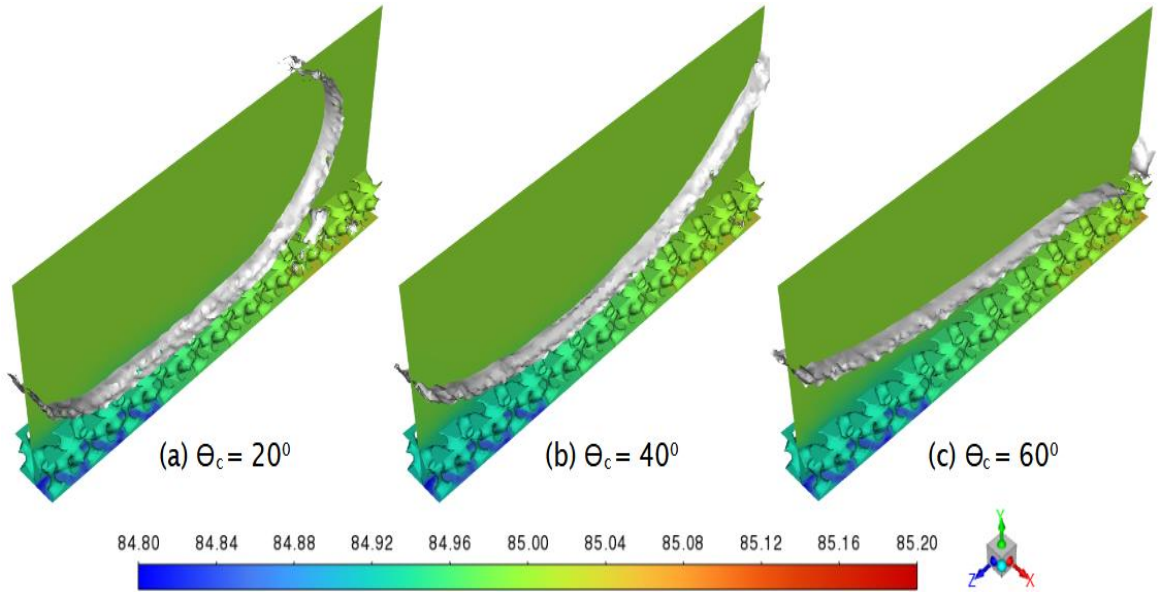

Figure 2: Contours of the temperature (in °C) superimposed by the liquid-vapour interface for three different contact angles after 1 sec.

3.2 Analysis

Fig. 3 shows two important quantities for analyzing performance of the heat pipe, i.e., volume of vapour generated and average temperature of the evaporator surface, as the time progressed. The lower value of contact angle is showing lesser vaporization as compared to the higher angles. As also seen in Fig. 2, the accumulation of the vapour is more towards the condenser and evaporator for 40 and 60 degrees, respectively; however, total vapour volume remains same. The temperature in the 60 degree case rises

gradually but also drops suddenly as the phase change starts and rapid evaporation takes place. No dry-out is observed in any case up to the duration shown.

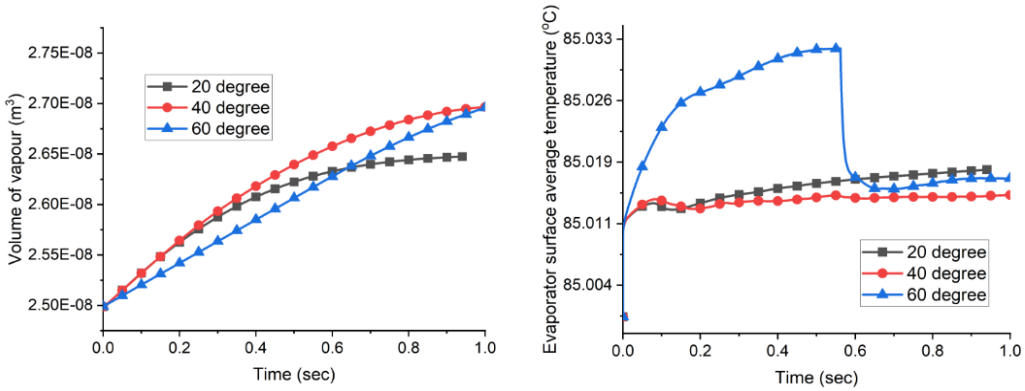

(a) Volume of vapour

(b) Average temperature of Evaporator surface

Figure 3: Plots showing the volume of vapour and average temperature of the evaporator surface up to 1 sec.

4 Conclusions

This study examines the influence of contact angle on the heat transfer efficacy of a rectangular heat pipe using TPMS lattice as a porous wick structure. The results presented here are limited to 1 second, whereas the equilibrium condition may require additional time to attain. On the basis of the conducted and presented research, the following conclusions could be drawn:

- The lower contact angle accumulates more liquid in the evaporator section, which is desirable because it frees up more space for the higher heating loads required for critical heat flux (CHF) applications. This phenomenon is suitable for overcoming two crucial limits, namely the heat pipe's capillary limit and boiling limit.
- The equilibrium condition is reached more rapidly when the contact angle is larger, which is adequate for overcoming the entrainment limit typically observed in heat pipes during initiation.

References

[1] D. Reay, R. McGlen, and P. Kew, *Heat pipes: theory, design and applications*. Butterworth-Heinemann, 2013.

[2] A. Faghri, "Review and advances in heat pipe science and technology," *J. Heat Transfer*, vol. 134, no. 12, 2012.

[3] C. W. Chan, E. Siqueiros, J. Ling-Chin, M. Royapoor, and A. P. Roskilly, "Heat utilisation technologies: A critical review of heat pipes," *Renew. Sustain. Energy Rev.*, vol. 50, pp. 615–627, 2015.

[4] M. A. Abdelkareem *et al.*, "Thermal management systems based on heat pipes for batteries in EVs/HEVs," *J. Energy Storage*, vol. 51, p. 104384, 2022.

[5] C. Guo, T. Wang, C. Guo, Y. Jiang, S. Tan, and Z. Li, "Effects of filling ratio, geometry parameters and coolant temperature on the heat transfer performance of a wraparound heat pipe," *Appl. Therm. Eng.*, vol. 200, p. 117724, 2022.